

Hybrid Simulations of beam-driven fishbone and TAEs in NSTX

G.Y. Fu^{1,2}, F. Wang^{1,3}, D.Y. Liu⁴

¹Princeton Plasma Physics Laboratory, Princeton, New Jersey, 08543, USA

²Zhejiang University, Institute for Fusion Theory and Simulation and Department of Physics Hangzhou, Zhejiang, 310027, China

³Key Laboratory of Materials Modification by Laser, Ion and Electron Beams (Ministry of Education), School of Physics and Optoelectronic Technology, Dalian University of Technology, Dalian 116024, China

⁴University of California, Irvine, CA, USA

E-mail: fu@pppl.gov

Abstract. Energetic particle modes and Alfvénic modes driven by super-Alfvénic beam ions were routinely observed in neutral beam heated plasmas on the National Spherical Torus Experiment (NSTX). These modes can significantly impact beam-ion transport, thus causing beam-ion redistribution and losses. In this paper we report on new self-consistent hybrid simulations of both fishbone instability and TAEs in NSTX plasmas using M3D-K code. First, linear simulations of beam-driven fishbone show that a new instability region appears for $q_{min} > 1.50$ when plasma toroidal rotation is included. The corresponding fishbone mode structure has strong ballooning feature. Both passing and trapped beam particles contribute to the instability drive. Nonlinear simulation shows strong mode frequency chirping as beam ion distribute is substantially redistributed in radial direction. It is found that trapped particles are mainly responsible for the nonlinear frequency chirping although passing particles' instability drive is comparable to that of trapped particles. Second, nonlinear simulations of multiple beam-driven TAEs and the n=1 fishbone have been carried out for the first time. The simulation results show strong interaction between multiple TAEs and fishbone that either enhances or reduces saturation level of individual modes due to overlap of wave particle resonances in phase space. Furthermore it is found that the mode saturation levels are very sensitive to q_{min} . When q_{min} drops below a critical value of about 1.19, the mode amplitudes increase sharply to large values. This result is similar to the observed transition to TAE avalanche in the late phase of NSTX discharges as q_{min} decreases in time.

1. Introduction

Energetic particle modes and Alfvénic modes driven by super-Alfvénic beam ions were routinely observed in neutral beam heated plasmas on the National Spherical Torus Experiment (NSTX). These modes can significantly impact beam-ion transport, thus causing beam-ion redistribution and losses. Recent simulation results with the kinetic/MHD hybrid code M3D-K[1, 2] show excitation and nonlinear saturation of $n=1$ fishbone with strong frequency chirping and beam ion radial profile flattening[3]. The linear simulation results of TAEs show mode radial structure consistent with the reflectometer measurements of electron density fluctuations[4]. In this paper we report on new self-consistent simulations of both fishbone instability and TAEs in NSTX plasmas. Our model is self-consistent with mode structure determined non-perturbatively including effects of energetic particles and plasma toroidal rotation.

2. Fishbone

This work extends the previous work[3] of $n=1$ mode simulation in NSTX to include the effects of finite toroidal rotation and detailed analysis of nonlinear dynamics of fishbone. The simulations in this study are also based on profiles and parameters of the NSTX discharge 124379 at $t = 0.635$ s. The profiles of pressure, energetic particles' pressure, safety factor (q) and toroidal rotation are shown in Fig. 1, where $\epsilon \equiv a/R_0 = 0.701$, $B_0 = 0.44$ T. The rotation profile and amplitude is chosen according to the experimental data with $v_{\phi,0} = 8.5 \times 10^4$ m/s. The fast ion distribution is a slowing-down in energy with a peaked distribution in pitch angle parameter:

$$F_0 = \frac{cH(E_{max} - E)}{E^{3/2} + E_c^{3/2}} e^{-\frac{(\Lambda - \Lambda_0)^2}{\Delta\Lambda^2}} e^{-\frac{\langle\psi\rangle}{\Delta\psi}}, \quad (1)$$

where c is a normalization factor, H is the step function. $E = v^2/2m_i + e\Phi$, where e is the particle charge and Φ is the electric potential associated with the plasma rotation. $E_{max} = v_0^2 m_i/2 + e\Phi$, where v_0 is the beam particle injection speed, and $E_c = v_c^2 m_i/2 + e\Phi$, where v_c is the critical velocity given by $v_c^3 \equiv 3\sqrt{\pi} m_e (2T_e/m_e)^{3/2}/m_i$, $\Lambda \equiv \mu B_0/E$ is the pitch angle parameter, where μ is the magnetic moment.

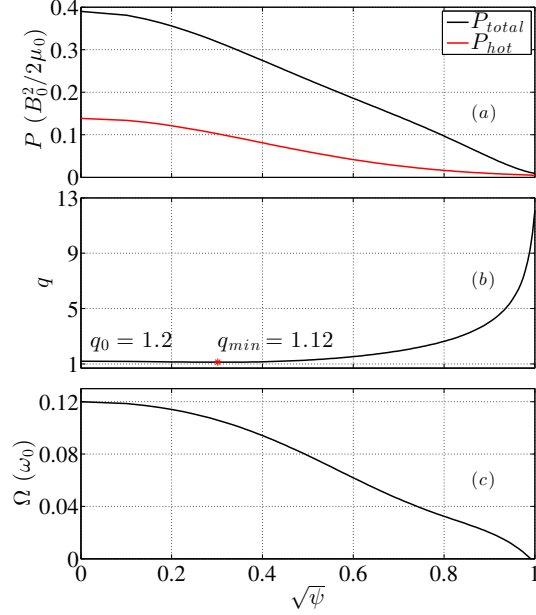


Figure 1. Equilibrium profiles vs. $\sqrt{\psi}$: (a) total pressure P_{total} , energetic particle pressure P_{hot} , (b) safety factor q , (c) toroidal rotation Ω .

ψ is normalized poloidal flux, and $\langle\psi\rangle$ is ψ averaged over particle orbit. The NBI injection energy of NSTX is 80 keV, the central pitch angle $\Lambda_0 = 0.6$, and $\Delta\Lambda = 0.3$, $\Delta\psi = 0.3$.

Linear simulations of beam-driven fishbone have been carried out based on parameters and profiles given above. Figure 2 shows the growth rate ($\gamma\tau_0$) and mode frequency (ω) as a function of q_{min} at $\beta_h/\beta_t = 0.35$, where $\tau_0 = R/v_A = 1.2$ μ s. The corresponding mode structures are shown in Fig. 3 for three values of q_{min} . We observe that effects of rotation are destabilizing. Specifically, a new unstable region at higher q_{min} (> 1.5) values appears due to the toroidal rotation. We also observe that the mode structure becomes ballooning as q_{min} increases. It is not totally clear why rotation destabilizes fishbone at high q_{min} . The sheared rotation can affect mode structure, beam ion drive and continuum damping. It can also affect beam ion resonance condition with finite orbit width. The sheared rotation can also affect significantly the

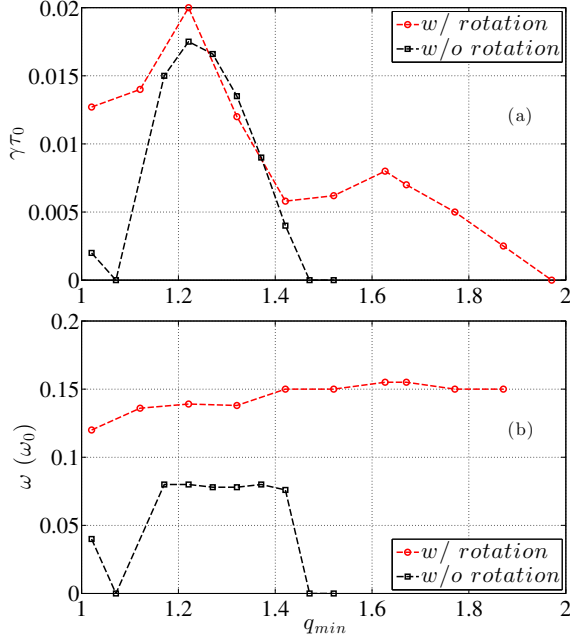


Figure 2. Linear growth rate (a) and mode frequency, (b) versus q_{min} with and without rotation, $\beta_h/\beta_t = 0.35$.

continuous spectrum which in turn can affect fishbone stability via its effects on mode structure, beam ion drive and continuum damping.

The instability drive of the fishbone is analyzed. In general, the mode is excited by free energy associated with radial gradient of beam ion distribution via wave particle resonant interaction. The resonance condition is given by

$$\omega = n\omega_\phi + p\omega_\theta, \quad n, p \in \mathbb{Z} \quad (2)$$

where p is an integer. For passing particles, ω_θ and ω_ϕ are particle poloidal and toroidal transit frequencies respectively. For trapped particles, ω_θ is the bounce frequency and $\omega_\phi \equiv \omega_d$ is the toroidal precession drift frequency. For typical parameters it is found that main resonances are $p=0$ due to trapped particles and $p=1$ due to passing particles. The relative contribution of trapped particles and passing particles to the fishbone drive are estimated by calculating each particle's energy change at the end of the linear simulation. It is found that passing particles' destabilizing contribution is comparable to the trapped particles'. For the specific case of $q_{min} = 1.321$ and $\beta_h/\beta_t = 0.2$, the passing particles' contribution is about 40% higher than the trapped particles'. This is quite different from fishbone instability in conventional tokamaks where the mode is driven mainly by either trapped or passing particles.

Now we investigate nonlinear evolution of chirping fishbone and associated dynamic behaviors of particles near resonances. The purpose is to understand

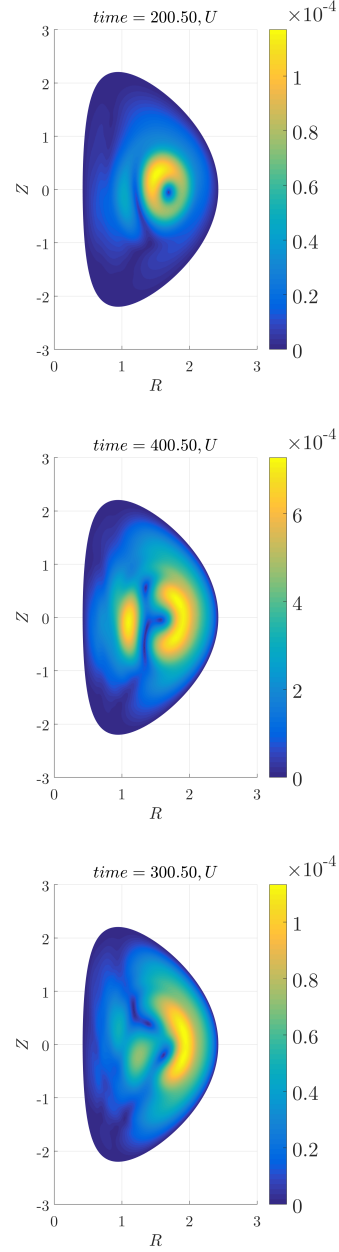


Figure 3. Linear mode structure (stream function U) with $q_{min} = 1.021, 1.321$ and 1.621 .

the chirping mechanism of beam-driven fishbone in spherical tokamaks. Figure 4 shows the nonlinear evolution of fishbone for a relatively low linear growth rate case with $\beta_h/\beta_t = 0.2$, and $q_{min} = 1.321$. The calculated linear mode frequency and growth rate is $\omega = 0.13 (\omega_0)$ and $\gamma\tau_0 = 0.005$. The figure shows time evolution of (a) \cos component of stream function U , here U is the stream function of the incompressional part of the perturbed plasma velocity, (b) mode frequency, (c) total energy changes of passing particles and trapped particles (positive means losing

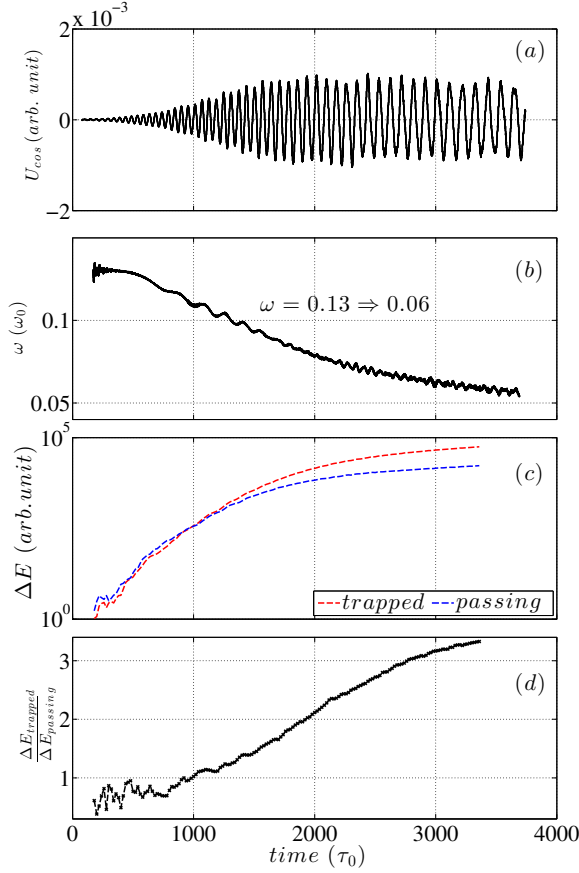


Figure 4. Nonlinear evolution of the fishbone mode: (a) the \cos component of U , (b) mode frequency, (c) energetic particles energy contribution from trapped and passing particles, (d) the ratio of trapped particles' energy contribution to passing particles'.

energy), and (d) ratio of the energy changes between trapped and passing particles. We observe that the mode saturates around $t \sim 1600 \tau_0$ and the mode amplitude persists thereafter. Correspondingly, the mode frequency chirps down strongly from $\omega = 0.13$ (ω_0) to $\omega = 0.06$ (ω_0). Interestingly, about half of the frequency drop occurs before the initial saturation. We also observe that, although the passing particle drive (measured by energy change) is somewhat larger than trapped particles' initially, the trapped particle drive become increasingly more important and dominant from $t \sim 1000 \tau_0$. This indicates that the chirping mode is driven mainly by trapped particles in the nonlinear phase. The corresponding beam ion distribution evolution is shown in Fig. 5 and Fig. 6 in 1D and 2D phase spaces at $t = 0, 1000, 2000$ and $3000 \tau_0$ respectively. Clearly, there is a large flattening region induced by both trapped and passing particles. Figure 5 shows the flattening region of the distribution function expands

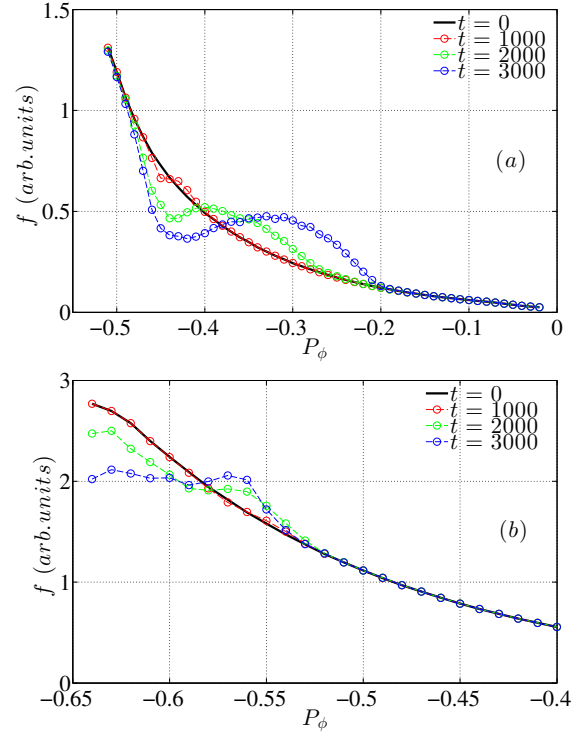


Figure 5. Distribution function in nonlinear evolution with $\mu \simeq 0.467$, (a) trapped particles with $E \simeq 0.406$ (E_0), (b) passing particles with $E \simeq 0.636$ (E_0).

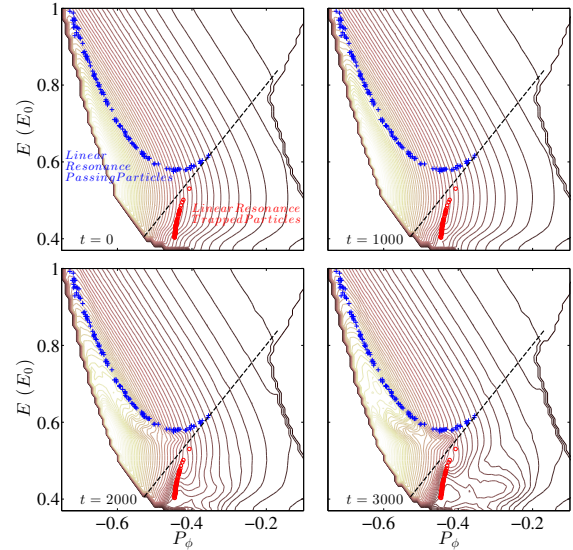


Figure 6. Distribution function at $t = 0, 1000, 2000$ and $3000 \tau_0$ with $\mu \simeq 0.467$.

outwards/inwards radially (or in P_ϕ space) in time for trapped/passing particles. For trapped particles, the center of the flattening region also move from the core to edge as the mode chirps down.

We now analyze the dynamics of resonant particles interacting with a chirping fishbone in order to understand the mechanism of fishbone nonlinear evolution including frequency chirping.

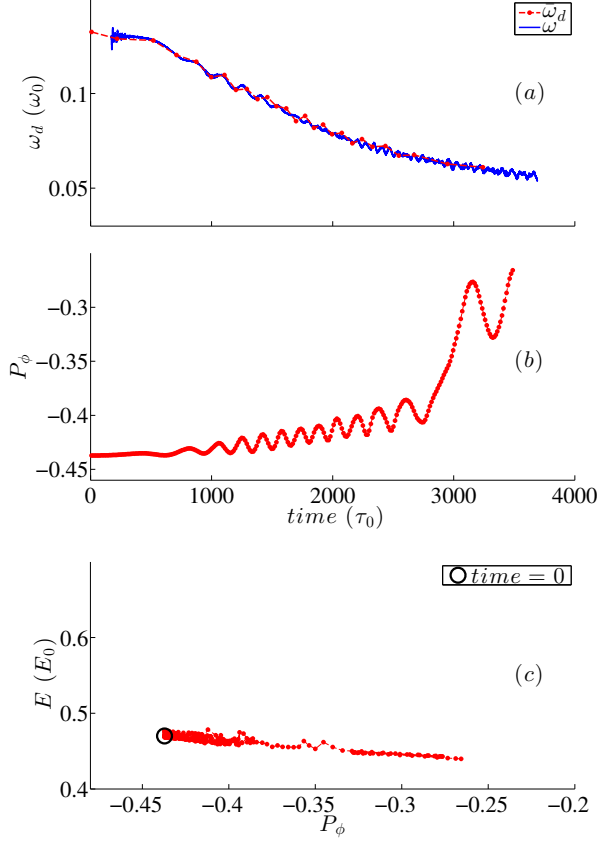


Figure 7. Nonlinear dynamic of trapped particle with $\omega_{d,t=0} \simeq \omega_{linear}$: (a) mode frequency, and ω_d ; (b) P_ϕ versus time; (c) particle's trajectory in P_ϕ and E spaces.

Figure 7 shows the evolution of precessional drift frequency ((a), red line), P_ϕ (b) and trajectory of a typical resonant trapped particle which is initially in resonance with the fishbone. The mode frequency evolution is also shown ((a), blue line). We observe that the particle keeps in resonance as the mode frequency chirps down. Correspondingly the particle moves outward radially as P_ϕ increases and energy decreases. The oscillation of P_ϕ in plot (b) indicates that the particle is trapped in the fishbone mode. The averaged value of P_ϕ increases at such rate that precessional frequency keeps in resonance with the chirping mode. We observe that almost all of these linear resonance trapped particles are phase-locked with the mode, and we plot only one of them to keep the plot clear. It is instructive to note that there is a big jump in P_ϕ and its oscillation amplitude at $t \sim 2800 \tau_0$ and $P_\phi \sim -0.4$. This is due to the

sudden change of the slope of function $\omega_d(P_\phi)$ near $P_\phi = -0.4$. It should be noted that these phase-locking resonant particles cause the radially expansion of beam ion redistribution as mode frequency chirps down (see Fig. 5).

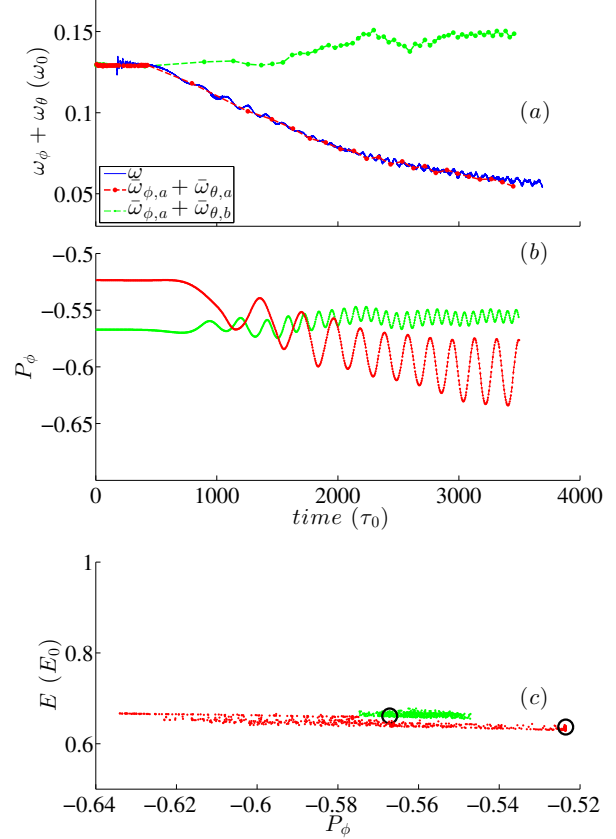


Figure 8. Nonlinear dynamic of passing particles with $\omega_{\phi,t=0} + \omega_{\theta,t=0} \simeq \omega_{linear}$.

We now look at the behavior of resonant passing particles. Figure 8 shows two typical passing particles nonlinear dynamic with initial frequency $\omega_{\phi,t=0} + \omega_{\theta,t=0} \simeq \omega_{linear}$. For orbit a (red lines), the particle keeps in resonance with the mode while the averaged P_ϕ decreases as the mode frequency chirps down. The direction of P_ϕ change is different from that of resonant trapped particles due to the opposite slopes of particle frequencies. As a result, the particle gets energy from the mode, in other words, it damps the mode nonlinearly. For orbit b (green lines), initially, the particle is in resonant. As the mode frequency chirps, the particle does not lock to the wave phase, in contrast, its frequency slightly increases, while energy decreases. At the end, it oscillates in a small range of P_ϕ and E spaces, but it still contribute energy to the mode on average. Furthermore, for either trapped or passing particles, a substantial fraction of initially

non-resonant particles become resonant particles and thus play a significant role in mode nonlinear drive and frequency chirping.

Now we can connect the nonlinear dynamics of single particle's orbit, distribution function and the mode together. For trapped particles, as the frequency chirps down, most of the linear resonances and near resonance particles are phase-locked with the wave, and they move radially and drive the mode continuously, which leads to distribution evolution in the phase space. For passing particles, there are also a fraction of particles keep in resonance nonlinearly. Due to the opposite slopes of the particle frequencies in P_ϕ space. They move from edge to core, and get energy from the mode. But there are more particles near resonance that are not phase-locked with the mode. They instead move from core to edge and drive the mode. These particles do not drive the mode continuously like trapped particles, but as the mode frequency chirping down and the resonance line for passing particles moving inwards, more and more particles can become resonant with the mode and drive the mode nonlinearly. Trapped particles provide the dominant driving force nonlinearly since the nonlinear driving trapped particles are phase-locked particles, and they increase in number as frequency chirps down and the mode amplitude growing.

It is instructive to compare our results of fishbone's chirping and particle dynamics with the Berk-Breizman's hole/clump theory of bump-on-tail instability[5, 6]. The theory shows that a hole/clump structure in distribution can develop from a near-threshold energetic particle-driven instability and the mode frequency chirps up/down while the hole/clump structure moves in phase spaces. Our results are consistent with the Berk-Breizman theory with respect to frequency chirping and associated resonant particle dynamics. In particular, our analysis shows that the resonant particles are trapped by the mode and thus they keep in resonance with the mode as frequency chirps down. Furthermore, a substantial fraction of initially non-resonant particles become resonant as the mode grows and frequency chirps down. This suggests formation of phase spaces island of resonant particles move in phase spaces as frequency chirps down. Our estimate shows that the adiabatic parameter $\alpha \equiv \frac{d\omega}{\omega_b^2 dt} \leq 0.005$ is very small where ω_b is the bounce frequency of a resonant particle trapped in the mode. This indicates that the adiabatic assumption of the Berk-Breizman theory is valid for our case. It should be noted that our results also differ from that of Berk-Breizman theory in important ways. The simulated evolution of beam ion distribution does not show a clear local hole/clump structure moving in phase spaces. Instead the beam ion redistribution is fairly

global. This is probably due to large oscillation of P_ϕ of resonant particles or large phase space island. It can be shown that a large island size can result from weak gradient of $\omega_d(P_\phi)$. Specifically an equation of motion for a resonant particle trapped in the finite amplitude fishbone mode can be derived to show that the corresponding oscillating amplitude of P_ϕ is inversely proportional to $\sqrt{|d\omega_d/dP_\phi|}$. Thus the width of phase space island of resonantly trapped particles is larger for smaller gradient of $\omega_d(P_\phi)$.

3. TAE

Previous linear simulations[4] showed that unstable TAEs with $n = 3, 4$, or 5 can be excited by the fast ions from neutral beam injection in NSTX. The simulated mode frequency, mode radial structure and phase shift were consistent with measurements from a multi-channel microwave reflectometer diagnostic. The simulations also showed that rotation can have a significant destabilizing effect when the rotation is comparable or larger than the experimental level. In this work, the previous linear study is extended to nonlinear regime to understand the physics of nonlinear saturation and multi-mode coupling. NSTX experimental results show that multiple low-amplitude beam-driven TAEs with weak frequency chirping can transit to mode avalanche with much larger amplitudes and strong frequency chirping. In order to explore mechanisms of avalanche, nonlinear simulations of multiple beam-driven TAEs and the $n=1$ fishbone have been carried out for the first time. The plasma parameters and profiles are based on the time slice of $t = 470$ of the NSTX discharge #141711 as in the previous study[4]. First we have carried out nonlinear simulations for a single TAE. The results show that the, for $n=2, 3$ or 4, the TAE saturates nonlinearly due to radially flattening of beam ion distribution. A modest frequency chirping range of about 10% to 20% is observed, consistent with quasi-steady state phase of TAE fluctuation observed before onset of TAE avalanche. Second, we have carried out multi-mode simulations with mode number $n = 1, 2, 3$ and 4 included simultaneously. The simulation results show strong interaction between TAEs and fishbone that either enhances or reduces saturation level of individual modes due to overlap of wave particle resonances in phase space. As beam ion beta increases beyond stability threshold, mode saturation levels are found to increase sharply. When beam ion beta exceeds some critical value, the locally flattening regions of beam ion distribution function merge together resulting in global particle transport and substantial particle loss. Furthermore it is found that the mode saturation levels are very sensitive to q_{min} . When q_{min} drops below

a critical value $q_{min} = 1.19$, the mode amplitudes increase sharply to large values. These results are similar to the observed transition to TAE avalanche in the later phase of the discharges as q_{min} drops in time in NSTX.

4. Summary

In summary we have carried out new self-consistent hybrid simulations of both fishbone instability and TAEs in NSTX plasmas using M3D-K code. First, linear simulations of beam-driven fishbone show that a new instability region appears for $q_{min} > 1.50$ when plasma toroidal rotation is included. The corresponding fishbone mode structure has strong ballooning feature. Both passing and trapped beam particles contribute to the instability drive. Nonlinear simulation shows strong mode frequency chirping as beam ion distribute is substantially redistributed in radial direction. It is found that trapped particles are mainly responsible for the nonlinear frequency chirping although passing particles' linear drive is comparable to that of trapped particles. Second, nonlinear simulations of multiple beam-driven TAEs and the $n = 1$ fishbone have been carried out for the first time. The simulation results show strong interaction between multiple TAEs and fishbone that either enhances or reduces saturation level of individual modes due to overlap of wave particle resonances in phase space. Furthermore it is found that the mode saturation levels are very sensitive to q_{min} . When q_{min} drops below a critical value of 1.19, the mode amplitudes increase sharply to large values. This result is similar to the observed transition to TAE avalanche in the later phase of NSTX discharges as q_{min} decreases in time.

Acknowledgments

This work is supported by the Department of Energy Scientific Discovery through Advanced Computing (SciDAC) under Grant No. DE-AC02-09CH11466, the National Natural Science Foundation of China under Grant No. 11505022, and China Postdoctoral Science Foundation under Grant No. 2014M561218. All this simulations were performed on super-computers at the National Energy Research Scientific Computing Center (NERSC). We thank Dr. Huishan Cai from University of Science and Technology of China), Dr. Mario Podesta and Dr. Nikolai Gorelenkov from Princeton Plasma Physics Laboratory for their valuable suggestions. And we also thanks Dr. Guangzhou Hao from University of California Irvine for his help about NSTX experimental data.

References

- [1] Park W. *et al. Phys. Plasmas*, 6(5):1796, 1999.
- [2] Fu G.Y. *et al. Phys. Plasmas*, 13(5):052517, 2006.
- [3] Wang F. *et al. Phys. Plasmas*, 20(10):102506, 2013.
- [4] Liu D. *et al. Phys. Plasmas*, 22(4):042509, 2015.
- [5] Berk H.L., Breizman B.N. and Petviashvili N.V. *Phys. Lett. A*, 234:213 1997; 238:408(E) 1998.
- [6] Berk H.L. *et al. Phys. Plasmas*, 6(8):3102, 1999